We are IntechOpen, the world's leading publisher of Open Access books Built by scientists, for scientists

4,800
Open access books available

122,000
International authors and editors

135M
Downloads

Our authors are among the

154
Countries delivered to

TOP 1%
most cited scientists

12.2%
Contributors from top 500 universities

CLARIVATE ANALYTICS BOOK CITATION INDEX INDEXED

WEB OF SCIENCE™

Selection of our books indexed in the Book Citation Index in Web of Science™ Core Collection (BKCI)

Interested in publishing with us?
Contact book.department@intechopen.com

Numbers displayed above are based on latest data collected.
For more information visit www.intechopen.com

Manipulator Design Strategy for a Specified Task Based on Human-Robot Collaboration

Seungnam Yu[a], Seungwhan Suh[a], Woonghee Son[b,c], Youngsoo Kim[b,d] and Changsoo Han[a]

[a] *Dept. of Mechanical Eng., Hanyang University, 1271 Sa-3 dong, Sangnok-gu, Ansan, Kyeonggi-do, Korea*

[b] *Dept. of Mechatronics Eng., Hanyang University, 1271 Sa-3 dong, Sangnok-gu, Ansan, Kyeonggi-do, Korea*

[c] *Korea Institute of Industrial Technology, 1271-18 Sa-3 dong, Sangnok-gu, Ansan, Kyeonggi-do, Korea*

[d] *Ministry of Education, Science and Technology, 77-6, Sejong-No, Jongno-Gu, Seoul, Korea*

1. Introduction

1.1 Overview and Motivation

This study starts from the improvement of developed curtain-wall installation robot.[1] Especially the robot was designed to handle a heavy weight curtain wall by integrating commercial excavator with custom-made manipulator system. Developed prototype system was tested in the real construction site and several considerations were deduced. First, separation of control source to operate the entire system is not good idea.

Fig. 1. Curtain-wall for skyscraper and developed curtain-wall installation robot system [1]

Second, hydraulic excavator can't exhibit the ideal performance on the curtain wall installation process because of its intrinsic jerking and shaking characteristics while handling the heavy weight materials.[2]

New research project is raised to solve those problems and to develop the useful automation system in real construction site. As a first step, the design process of scale down manipulator is proposed to ease the kinematical robot design. This scaled down robot and corresponding assumptions are applied to the simulation and comparison works of each robot design candidate. Then, the target task is selected as curtain wall installation which is required 6-DOF motion to cover the whole installation process. As abovementioned, this study based on the modification of prototype system hence end-effector of prototype system is utilized continuously and focused to develop the arm part except the wrist part. Therefore, the final goal of this study is to propose the proper design of robot manipulator handled by human passively as man-machine cooperation system specialized to curtain wall installation process. This idea is not only applied to passive system but also active controlled system because newly modified design makes to promote the physical performance of manipulator system intrinsically.
This work primarily focuses on selection of optimal type of joint type and link length considering task type and motion requirements. The developments of this work provide an open and objective design and analysis framework for a serial robot. This framework may be applied at any stage in the design process. As abovementioned, this study applies this frame work to prototype of our curtain wall installation robot and modified its kinematic design.

1.2 Experimental analysis of prototype system

Originally developed curtain wall installation system is combined by two modules, one is general commercial excavator and the other is newly designed 3-DOF manipulator. That system is tested in the real construction site by a new installation task scenario and compared with conventional installation task operated by human. Fig.2 shows the task results of curtain wall installation task. As the result, Robot requires more time than human for same task! Throughout this test, several considerations for the prototype system are deduced

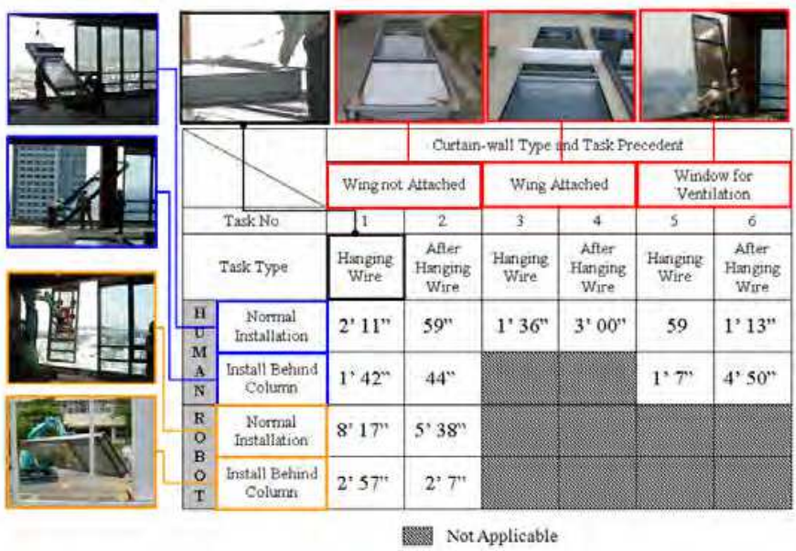

		Curtain-wall Type and Task Precedent					
		Wing not Attached		Wing Attached		Window for Ventilation	
Task No		1	2	3	4	5	6
Task Type		Hanging Wire	After Hanging Wire	Hanging Wire	After Hanging Wire	Hanging Wire	After Hanging Wire
HUMAN	Normal Installation	2' 11"	59"	1' 36"	3' 00"	59	1' 13"
	Install Behind Column	1' 42"	44"			1' 7"	4' 50"
ROBOT	Normal Installation	8' 17"	5' 38"				
	Install Behind Column	2' 57"	2' 7"				

Not Applicable

Fig. 2. Field test of curtain wall installation robot and its elapsed time for each process [3]

First, 2-way control strategy of Excavator and 3-DOF manipulator is not efficient because it is hard to operate excavator boom and 3-DOF manipulator simultaneously through whole installation process. That is, the tasks of the two machines could not be completed independently hence the two workers had to work simultaneously. (Fig.3)
Second, using excavator for delicate motion is not appropriate. Excavator is not a machine for material handling but digging a ground. That hydraulic system has the leakage and drooping characteristics. Therefore, it is difficult to handle the heavy curtain wall and assembly it on the slot gently.
Based on those considerations, new concept for manipulator design for man-machine collaboration is proposed.

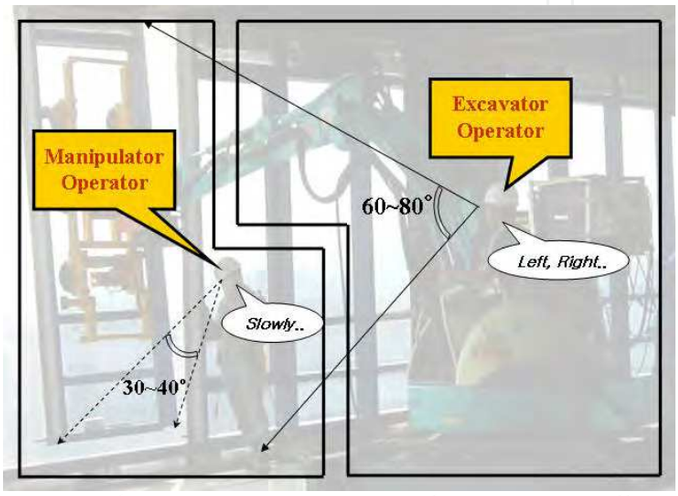

Fig. 3. Communication confusion in cooperative work in curtain wall installation

1.3 Conceptual design of new system

Final goal of this research is dedicated to man-machine cooperation system. That is the hybrid system that mixes the sensitivity of human and high performance of machine. This system is powerful at a field area. There is, unlike factory, not arranged and materials which handled by machine are relatively low standard one. Most of all, those materials are very heavy and large! Therefore, it is hard to automate the whole task using the robot and automation system.
Human sense is very useful in that case. Through this entire research is dedicated to the development of manipulator which handled by human and especially the major issue is to decide the adequate kinematical combination of manipulator components through the simulation of scale down manipulator of real one. Fig.4 shows the considerations for new manipulator design and Fig.5 describes concept of the intuitive curtain wall installation robot derived by upper considerations and its simulation strategy.

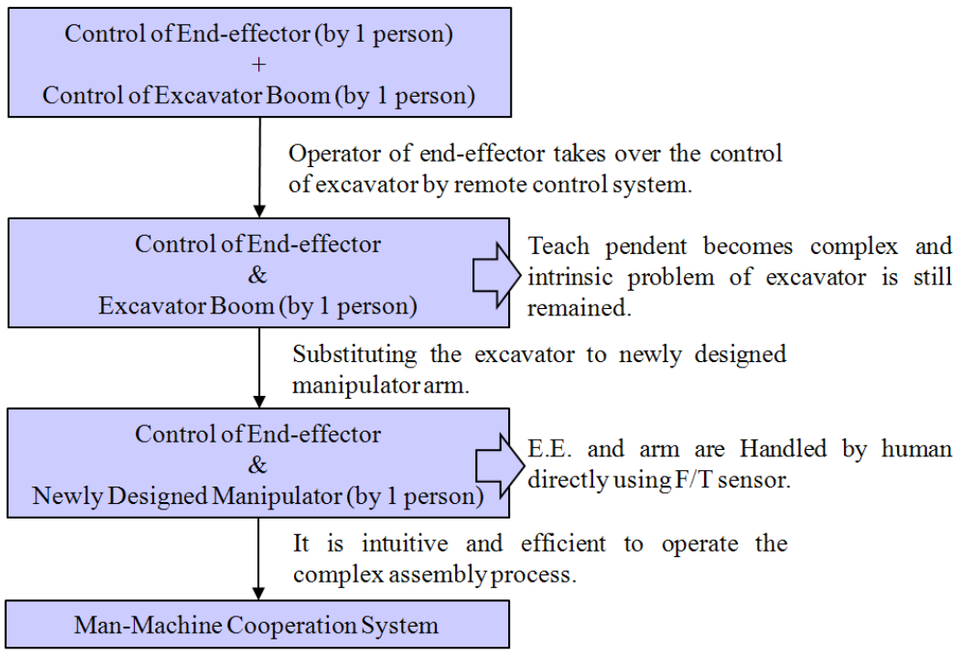

Fig. 4. Considerations for new mechanism

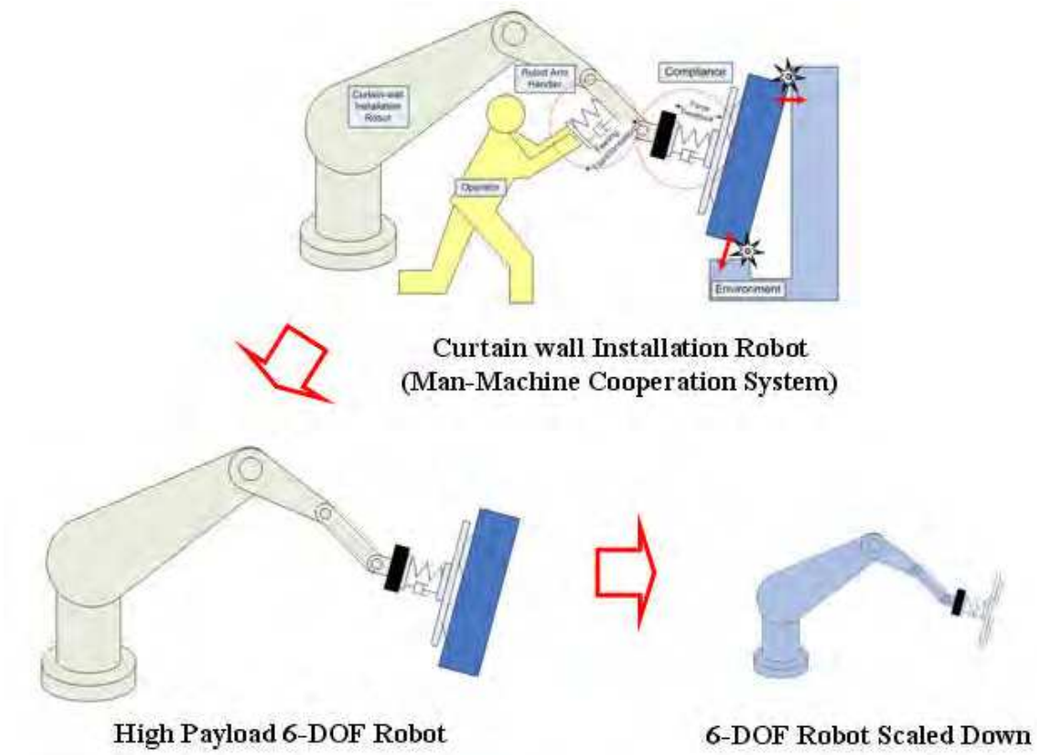

Fig. 5. Scaled Down Manipulator for Specified Robot Manipulator Design

1.4 Basic Assumptions for Specified Manipulator Design

1.4.1 Invariant part of proposed manipulator system

To design the modified manipulator, the several invariant parts are considered. First part is DOF of end-effecter. It is designed by analysis of conventional process of curtain wall installation (Fig.6(a)) and as shown in Fig.6(b), R-R-P type end-effector is developed. New design for manipulator system is focused to arm part integrating with this end-effector.

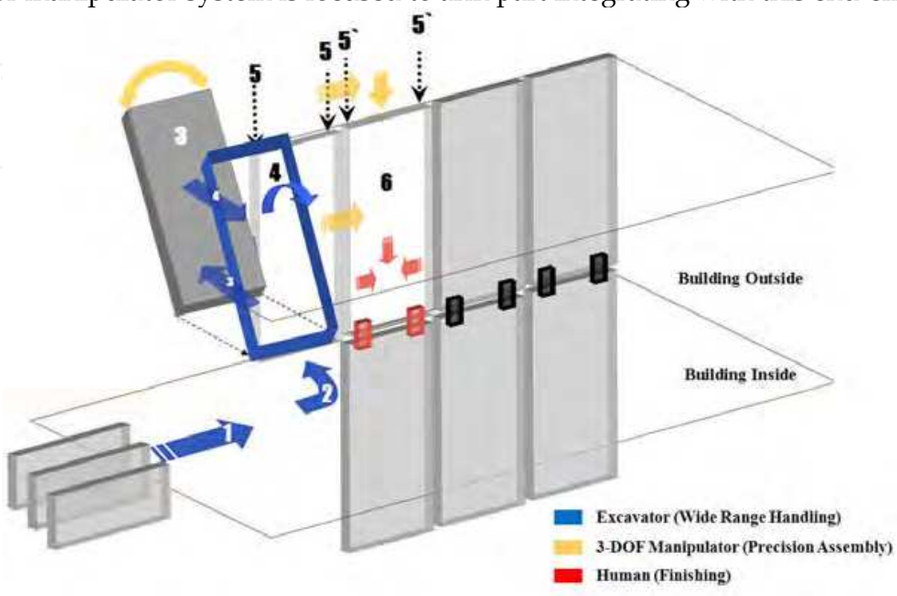

(a) Curtain wall Installation Process

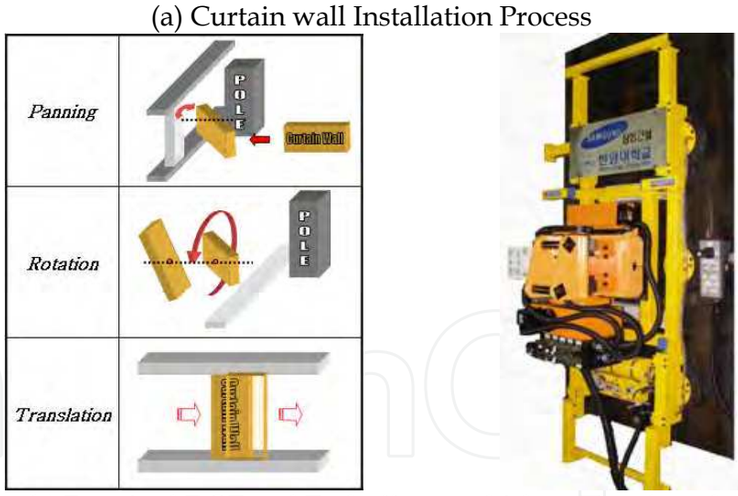

(b) Required DOF and End-effecter which we developed

Fig. 6. Invariant Condition - DOF of End effecter [1]

1.4.2 Variant part of proposed manipulator system

Variant part of the newly designed manipulator system is mainly arm part. Finally, joint of base frame, shoulder joint and elbow joint are remained except the invariant elements. Therefore, this research process can be simplified to find a combination of joint type of three joints and link ratio of upper and lower arm. Detailed assumptions for this study are as follows.

1. Each joint of manipulator is actuated by its own general actuators.
2. To cover the working area, one revolute joint which axis is perpendicular to the ground is should be included.
3. Each joint has one DOF and revolute joint and prismatic joint are considered only.
4. Target task is performed by nearly full stretched manipulator (generally, this task is performed in the skyscraper hence safety is most important issue) and manipulator is handled by human operator directly.

2. Selection of Adequate Joint Combination

2.1 Comparison of the basic kinematics of R-R type and R-P type

2.1.1 Simulation Conditions

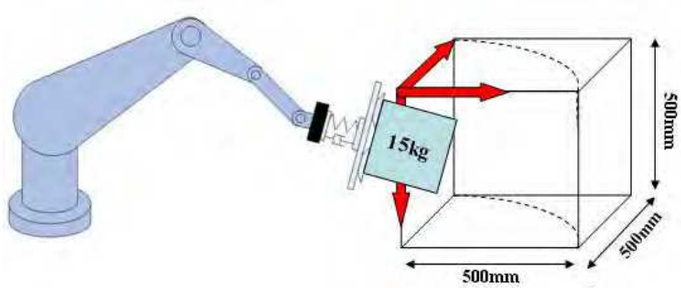

Fig. 7. Motion Range of 6-DOF Scaled Down

First, to select the part of shoulder joint and elbow joint, the motion range of manipulators is considered to 500mm×500mm×500mm, and link length of each manipulator is fixed by $l_1 = 300mm,\ l_2 = 330mm$. This process is dedicated to compare the performance of R-P and R-R type manipulator. Table.1 shows the several conditions for this simulation.

R-R Type	Contents	R-P Type
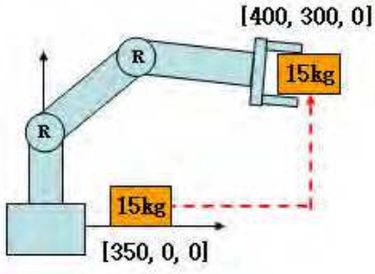	[Task definition] : In X-Y plane, 15kg weight box is moved initial pt. to final pt. through same trajectory	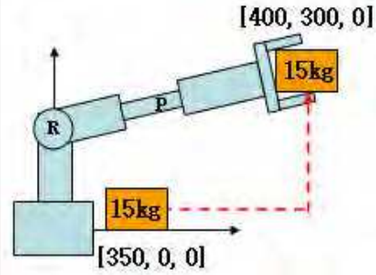
[350,0,0]	Initial Position	[350,0,0]
[400,300,0]	Final Position	[400,300,0]
$l_1 = 300mm,\ l_2 = 330mm$	Link Length	$l_1 = 300mm$ $0 \le d_2 \le 350mm$

Table. 1. Experimental Condition of two joint types of manipulators

2.1.2 Basic kinematics

2.1.2.1 R-R Type Manipulator

Table 2 shows the DH table[4] of R-R type manipulator.

	α_i	a_i	d_i	θ_i
1	0	0	0	θ_1
2	0	l_1	0	θ_2
3	0	l_2	0	0

Table. 2. DH table of R-R type manipulator

Using the upper information, transformation matrix and position vector of end effecter can be calculated. (l_1, l_2 is link length, and $s_1 = \sin\theta_1$, $c_1 = \cos\theta_1$)

Transformation matrix,

$$ {}^{0}_{E}T = \begin{bmatrix} c_{12} & -s_{12} & 0 & l_1c_1 + l_2c_{12} \\ s_{12} & c_{12} & 0 & l_1s_1 + l_2s_{12} \\ 0 & 0 & 1 & 0 \\ 0 & 0 & 0 & 1 \end{bmatrix} \tag{1} $$

Position vector of End effecter

$$ {}^{0}P_{E-E} = \begin{bmatrix} l_1c_1 + l_2c_{12} \\ l_1s_1 + l_2s_{12} \\ 0 \end{bmatrix} \tag{2} $$

Using Cramer rule,

$$ c_2 = \frac{x^2 + y^2 - l_1^2 - l_2^2}{2l_1l_2}, \quad s_2 = \pm\sqrt{1 - c_2^2} \tag{3} $$

Thus, manipulator pose at the initial position is $\theta_2 = -112.70,\ \theta_1 = 60.44$, and pose at the final position is $\theta_2 = -75.04,\ \theta_1 = 76.48$.

Jacobian and Hessian matrix is as follows,

$$ \begin{bmatrix} \dot{x} \\ \dot{y} \end{bmatrix} = \begin{bmatrix} -l_1s_1 - l_2s_{12} & -l_2s_{12} \\ l_1c_1 + l_2c_{12} & l_2c_{12} \end{bmatrix} \begin{bmatrix} \dot{\theta}_1 \\ \dot{\theta}_2 \end{bmatrix} \tag{4} $$

$$\left[H^u_{\phi\phi}\right]_{1;;} = \begin{bmatrix} \frac{\partial}{\partial\phi_1}\left[G^u_\phi\right]^x \\ \frac{\partial}{\partial\phi_2}\left[G^u_\phi\right]^x \end{bmatrix} = \begin{bmatrix} -l_1c_1 - l_2c_{12} & -l_2c_{12} \\ -l_2c_{12} & -l_2c_{12} \end{bmatrix}$$
$$\left[H^u_{\phi\phi}\right]_{2;;} = \begin{bmatrix} \frac{\partial}{\partial\phi_1}\left[G^u_\phi\right]^y \\ \frac{\partial}{\partial\phi_2}\left[G^u_\phi\right]^y \end{bmatrix} = \begin{bmatrix} -l_1s_1 - l_2s_{12} & -l_2s_{12} \\ -l_2s_{12} & -l_2s_{12} \end{bmatrix} \quad (5)$$

2.1.2.2 R-P Type Manipulator

Table.3 represents the DH table of R-P type manipulator.

	α_i	a_i	d_i	θ_i
1	0	0	0	$\theta_1 + \frac{\pi}{2}$
2	$\frac{\pi}{2}$	0	d_2	θ_2
3	0	0	l_1	0

Table. 3. DH table of R-P type manipulator

Likewise, transformation matrix, position vector of End effecter, Jacobian and Hessian of R-P type can be derived.

Transformation matrix is,

$${}^0_E T = \begin{bmatrix} -s_1 & 0 & c_1 & (l_1+d)c_1 \\ c_1 & 0 & s_1 & (l_1+d)s_1 \\ 0 & 1 & 0 & 0 \\ 0 & 0 & 0 & 1 \end{bmatrix} \quad (6)$$

Position vector of End effecter

$${}^0P_{E-E} = \begin{bmatrix} (l_1+d)c_1 \\ (l_1+d)s_1 \\ 0 \end{bmatrix} \quad (7)$$

Jacobian and Hessian of R-P type are as follows

$$\begin{bmatrix} \dot{x} \\ \dot{y} \end{bmatrix} = \begin{bmatrix} -(l_1+d)s_1 & c_1 \\ (l_1+d)c_1 & s_1 \end{bmatrix} \begin{bmatrix} \dot{\theta}_1 \\ \dot{d} \end{bmatrix} \quad (8)$$

$$\left[H^u_{\phi\phi}\right]_{1;;} = \begin{bmatrix} \frac{\partial}{\partial\phi_1}\left[G^u_\phi\right]^x \\ \frac{\partial}{\partial\phi_2}\left[G^u_\phi\right]^x \end{bmatrix} = \begin{bmatrix} -(l_1+d)c_1 & -s_1 \\ -c_1 & 0 \end{bmatrix}$$
$$\left[H^u_{\phi\phi}\right]_{2;;} = \begin{bmatrix} \frac{\partial}{\partial\phi_1}\left[G^u_\phi\right]^y \\ \frac{\partial}{\partial\phi_2}\left[G^u_\phi\right]^y \end{bmatrix} = \begin{bmatrix} -(l_1+d)s_1 & c_1 \\ c_1 & 0 \end{bmatrix} \quad (9)$$

2.1.3 Performance Analysis

2.1.3.1 Required torque

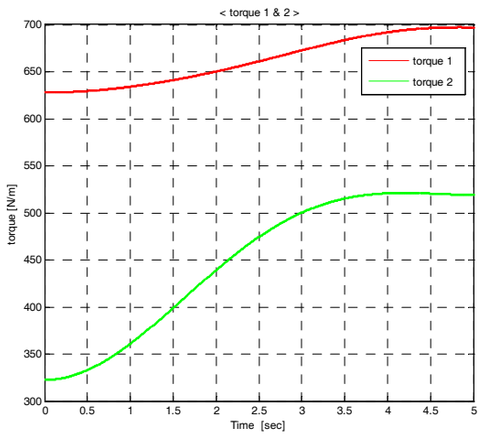

RR type

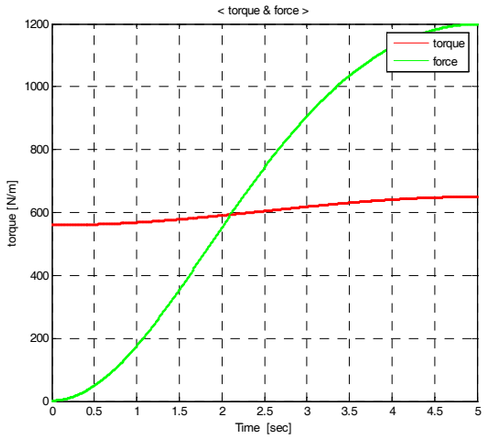

RP type

Min. Torque 1: 628.2526 Min. Torque2: 322.8128 Max. Torque 1: 697.2908 Max. Torque 2: 521.3266	Min. Torque 1: 560.9 Min. Force 2: 2.4696 Max. Torque 1: 649.8 Max. Force 2: 1199.2

Table. 4. Required torque of each type of manipulator

Required torque of each joint combination is calculated as shown in Table.4. Required torques of each joint is almost same but performance of prismatic joint of R-P type changes more rapidly.

2.1.3.2 Force Transmission Ratio (FTR)

Force transmission is important index to verify manipulator performance as changes of manipulator pose. The following equation represents force transmission ratio.[5]

$$\text{Force transmission ratio} = \frac{1}{(\text{Min. eigenvalue of Jacobian})} \tag{10}$$

$$\tau = \mathrm{J}^{\mathrm{T}} f$$

In this simulation, the reach of manipulator is increasing by time. As shown in Fig.8, R-P type has better performance when the reach of manipulator is increased. It can be observed from the simulation results that when the reach of R-R type manipulator becomes larger, the force transmission ratios become smaller. Specifically, manipulator pose are placed on last position, the force transmission ratio of R-P type becomes three times of FTR of R-R type.

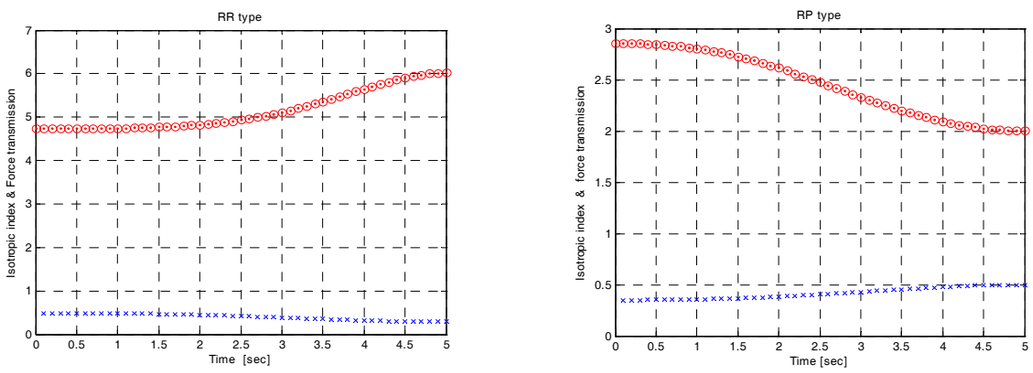

(a) R-R type (b) R-P type

Fig. 8. Force Transmission Ratio of R-R type and R-P type
(Isotropic Index: Upper line, FTR: Lower Line)

2.2 Comparison of Computation Complexities

2.2.1 Three DOF Planar manipulator

Expanding the considerations of previous chapter, combination of three joints including base frame is considered. This concept is illustrated with the 3-DOF planar and spatial robots with two revolute and one prismatic joint. This provides the most economic computational counts.

Based on the model given by eq. (11) and (12), computational complexities for the GIM and MCI of an n-link, n-revolute joint serial robot can be computed. GIM means complexities Index for Generalized Inertia Matrix and MCI means Matrix of Convective Inertia. [6]

$$GIM : (3.5n^2 + 11.5n - 7)M(2n^2 + 9n - 7)A \tag{11}$$

$$MCI : (7n^2 + 13n + 4)M(4n^2 + 13n + 2)A \tag{12}$$

Table.5 represents computation complexities of 3-DOF planar manipulator calculated by eq. (11) and (12). As shown in Table.5, R-P-R type has minimum value for the GIM

Computation and P-R-R type has minimum value for the MCI computation.

Type	GIM Computation	MCI Computation	Total
R-R-P	46M; 29A	76M; 42A	122M; 71A
R-P-R	34M; 22A	88M; 39A	122M; 61A
P-R-R	42M; 27A	53M; 29A	96M; 56A

Table. 5. Computation Complexities of 3-DOF Planar manipulator

2.2.2 Three DOF Spatial manipulator

3-DOF spatial manipulator has an eq. of GIM and MCI as follows.

$$GIM : (11n^2 + 34n - 18)M \ (7n^2 + 37n - 18)A \tag{13}$$

$$MCI : (14n^2 + 22n + 4)M \ (13.5n^2 + 55.5n - 65.5)A \tag{14}$$

Note that the GIM complexity is less than the value reported by Walker and Orin (1982),i.e. $(12n^2 + 56n - 27)M \quad (7n^2 + 67n - 53)A$, whereas for MCI complexity value is not available for comparison.[6] Three-DOF spatial robot arms with two revolute and one prismatic joint are shown in Fig.9(a)-(c).

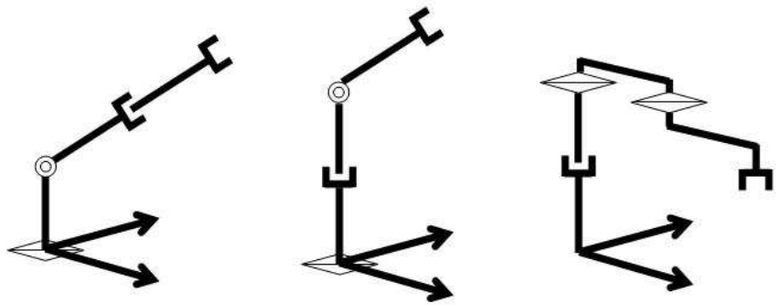

(a) R-R-P (b) R-P-R (c) P-R-R

Fig. 9. Three Types of Spatial manipulator

Two of which, namely, those in Fig.9(a) and (c) are the Stanford and RTX robot arms, respectively. While the Stanford arm has spherical workspace, RTX is of SCARA type. Computational complexities for the Generalized Inertia Matrix (GIM) and Matrix of Convective Inertia (MCI) terms for all these robot arms are tabulated in Table.6 which are based on eq. (13) and (14). Similar to the planar case, simplicity due to the orthogonal positions of the joint axes is also taken into account. Based on the total minimum computational complexity P-R-R configuration (RTX Robot), shown in Fig.9(c) has minimum computation complexities.

Type	GIM Computation	MCI Computation	Total
R-R-P	170M 154A	522M 352A	692M 506A
R-P-R	153M 148A	556M 415A	709M 583A
P-R-R	142M 138A	389M 317A	531M 455A

Table. 6. Computation Complexities of 3-DOF Spatial manipulator [6]

2.3 Comparison of Manipulability

2.3.1 Basic Formulations

Manipulability is the ability to reach a certain position or set of positions, and to change the position or orientation at a given configuration. This performance index is most general one, and it's possible to map on the workspace of a manipulator. Commonly, manipulability can be expressed following equations.[7]

$$W = \sqrt{\det(JJ^T)} \tag{15}$$

$$W = \left|\det(J)\right| = \sqrt{\lambda_1\lambda_2.....\lambda_m} = \sigma_1\sigma_2.....\sigma_m \tag{16}$$

Where, $\lambda_1 \geq \lambda_2 \geq ..... \geq \lambda_m \geq 0$ are Eigen values of JJ^T and $\sigma_1 \geq \sigma_2 \geq ..... \geq \sigma_m \geq 0 \quad (\sigma_i = \sqrt{\lambda_i})$ are singular values of Jacobian matrix. Manipulability becomes equal to zero if and only if manipulability Space becomes less than m. That is singular point.

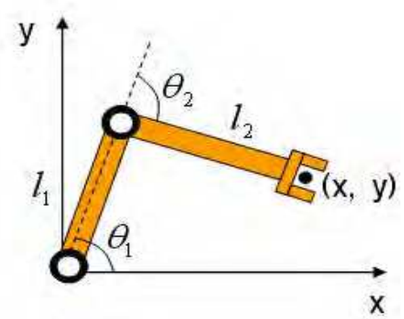

Fig. 10. Generalized 2-DOF R-R type Manipulator

Jacobian matrix of manipulator of Fig.10 is like eq. (17).

$$J(\theta) = \begin{pmatrix} l_1c_1 + l_2c_{12} & l_2c_{12} \\ -l_1s_1 - l_2s_{12} & -l_2s_{12} \end{pmatrix} \tag{17}$$

$$W = \left|\det J(\theta)\right| = l_1l_2\left|\sin\theta_2\right| \tag{18}$$

When $\theta_2 = \pm\frac{\pi}{2}$, the configuration of the Manipulator is Optimal ($l_1 + l_2 = C$; C is constant). As a result, the optimal design of link length is $l_1 = l_2$. And optimal configuration is

$$\theta_2 = \pm\frac{\pi}{2}.$$

2.3.2 Manipulability Ellipsoid Analysis

It is natural to use the determinant of the Jacobian in a measure of manipulator dexterity. Manipulator Ellipsoid shows the manipulability of each manipulator by a shape of ellipsoid. That is, more closer to a complete circle, the manipulator has better manipulability. To calculate the manipulability ellipsoid, institute new matrices.

$$V = J(\theta)\dot{\theta} \tag{19}$$

$$J = Q_1 \Sigma Q_2^T \tag{20}$$

To verify the performance of manipulator in a workspace, generally this index is plotted to the workspace, and considers the phase of change of this index. In this study, the case which optimal link length is $l_1 = l_2$ is considered, and compared with the case which link length is different each other.

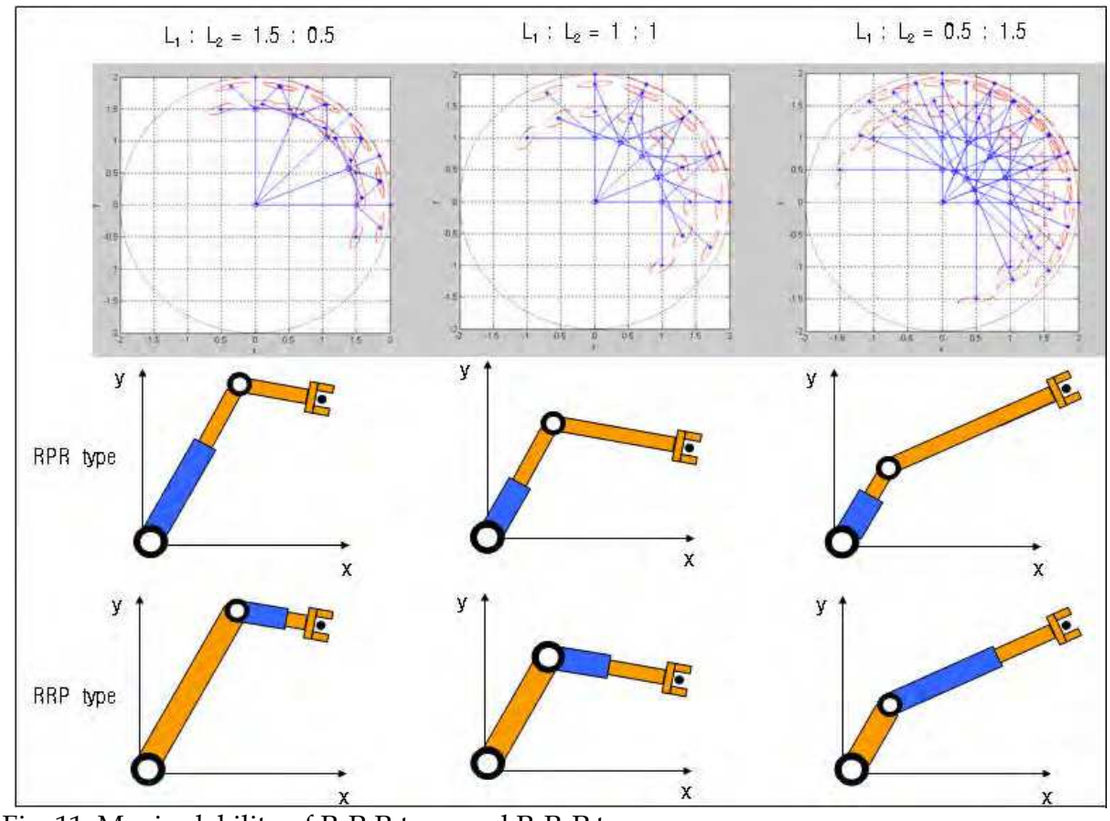

Fig. 11. Manipulability of R-P-R type and R-R-P type

Fig.11 represents manipulability ellipsoid of R-P-R and R-R-P type. First column is the case of link length 3:1 ratio, second column is the case of 1:1 ratio and last case shows the case of 1:3 ratio. This figure shows link length of lower arm becomes larger, and then the area of ellipsoid of near the outer line becomes larger. This means better design that the length of lower arm becomes larger than upper arm for the specific task which this study concerns.

2.4 Comparison of Motion Capability

2.4.1 Motion Capability of R-R-R type

The motion capability of the manipulator is defined to be the measure or volume of subset of all possible rotations and translations of rigid body. The technique that will be used is similar to that of calculating the volume of a region in R^3 by integrating the volume element $dV = dxdydz$ over the region of concern. The first application of the volume element to robotics appears in Karger (1989). It is also briefly mentioned as a possible area of study in Loncaric (1985). [8]

First, applying the volume element to a manipulator capable of both rotational and translation motion, it may be instructive to investigate the simple case of planar motion.

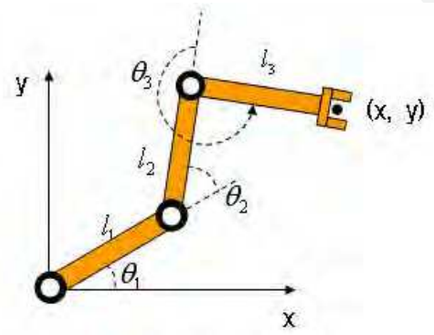

Fig. 12. R-R-R Type Planar Manipulator

If the planar R-R-R type manipulator shown in Fig.12 is considered, the problem reduces to reparameterizing the manifold $R^2 \times 2\pi$ in terms of the joint angles. This is accomplished via the forward analysis for the mechanism and yields

$$\begin{aligned} x &= l_1 \cos\theta_1 + l_2 \cos(\theta_1 + \theta_2) + l_3 \cos(\theta_1 + \theta_2 + \theta_3) \\ y &= l_1 \sin\theta_1 + l_2 \sin(\theta_1 + \theta_2) + l_3 \sin(\theta_1 + \theta_2 + \theta_3) \\ \theta &= \theta_1 + \theta_2 + \theta_3 \end{aligned} \tag{21}$$

The coordinate-induced tangent vectors are then given by

$$\begin{bmatrix} t_{\theta_1} \\ t_{\theta_2} \\ t_{\theta_3} \end{bmatrix} = \begin{bmatrix} \frac{\partial x}{\partial \theta_1} & \frac{\partial y}{\partial \theta_1} & \frac{\partial \theta}{\partial \theta_1} \\ \frac{\partial x}{\partial \theta_2} & \frac{\partial y}{\partial \theta_2} & \frac{\partial \theta}{\partial \theta_2} \\ \frac{\partial x}{\partial \theta_3} & \frac{\partial y}{\partial \theta_3} & \frac{\partial \theta}{\partial \theta_3} \end{bmatrix} \begin{bmatrix} t_x \\ t_y \\ t_\theta \end{bmatrix} \tag{22}$$

This equation can be described by following equation.

$$t_{\theta_1} = \begin{bmatrix} -l_1 \sin(\theta_1) - l_2 \sin(\theta_1 + \theta_2) - l_3 \sin(\theta_1 + \theta_2 + \theta_3) \\ l_1 \cos(\theta_1) + l_2 \cos(\theta_1 + \theta_2) + l_3 \cos(\theta_1 + \theta_2 + \theta_3) \\ 1 \end{bmatrix} \tag{23}$$

$$t_{\theta_2} = \begin{bmatrix} -l_2 \sin(\theta_1 + \theta_2) - l_3 \sin(\theta_1 + \theta_2 + \theta_3) \\ l_2 \cos(\theta_1 + \theta_2) + l_3 \cos(\theta_1 + \theta_2 + \theta_3) \\ 1 \end{bmatrix} \tag{24}$$

$$t_{\theta_3} = \begin{bmatrix} -l_3 \sin(\theta_1 + \theta_2 + \theta_3) \\ l_3 \cos(\theta_1 + \theta_2 + \theta_3) \\ 1 \end{bmatrix} \tag{25}$$

The magnitude of the volume of the parallelepiped formed by these tangent vectors is given by

$$\begin{vmatrix} t_{\theta_1} \cdot t_{\theta_1} & t_{\theta_1} \cdot t_{\theta_2} & t_{\theta_1} \cdot t_{\theta_3} \\ t_{\theta_2} \cdot t_{\theta_1} & t_{\theta_2} \cdot t_{\theta_2} & t_{\theta_2} \cdot t_{\theta_3} \\ t_{\theta_3} \cdot t_{\theta_1} & t_{\theta_3} \cdot t_{\theta_2} & t_{\theta_3} \cdot t_{\theta_3} \end{vmatrix}^{\frac{1}{2}} = l_1 l_2 \left| \sin \theta_2 \right| \tag{26}$$

Each element of this matrix represents the standard dot product which is given by $v \cdot w = |v||w| \cos\theta$. Hence, the volume element, in terms of the joint angle parameterization, is given by

$$dV = l_1 l_2 \left| \sin \theta_2 \right| d\theta_1 d\theta_2 d\theta_3 \tag{27}$$

The tangent vector represents the instantaneous motions of the end effecter. Hence the loss of one or more of these vectors represents a loss in a degree of freedom, and the volume element degenerates when the robot is in a singularity configuration. The volume, or what will be referred to as the motion capability, achieved by the robot, assuming all joints can rotate $2\pi \; radian$, is given by

$$\begin{aligned} V &= \int_{\theta_1=0}^{2\pi} \int_{\theta_2=0}^{2\pi} \int_{\theta_3=0}^{2\pi} l_1 l_2 \left| \sin \theta_2 \right| d\theta_1 d\theta_2 d\theta_3 \\ &= 16\pi^2 l_1 l_2 \end{aligned} \tag{28}$$

$$V = 16\pi^2 l_1 l_2 = 4\pi \times [\pi (l_1 + l_2)^2 - \pi (l_1 - l_2)^2] \tag{29}$$

In the case of R-R-R type manipulator, motion capability is 4π times of physical workspace. Adding to this, consider the other types of manipulator. In addition to this type, we will consider other type of manipulator. Second type is R-P-R type (Fig.13).

2.4.2 Motion Capability of R-P-R type

Likewise, volume element and motion capability can be calculated.

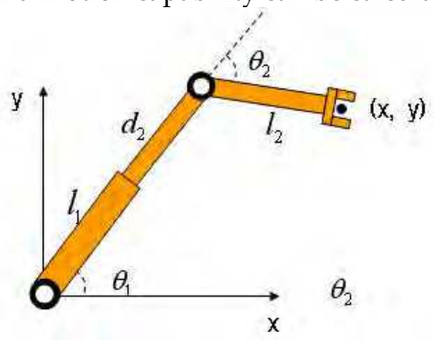

Fig. 13. R-P-R type manipulator

$$\begin{aligned} x &= l_1 \cos\theta_1 + d_1 \cos\theta_1 + l_2 \cos\theta_2 \\ y &= l_1 \sin\theta_1 + d_1 \sin\theta_1 + l_2 \sin\theta_2 \\ \theta &= \theta_1 + \theta_2 \end{aligned} \tag{30}$$

$$t_{\theta_1} = \begin{bmatrix} -(l_1 + d_1)\sin(\theta_1) \\ (l_1 + d_1)\cos(\theta_1) \\ 1 \end{bmatrix} \tag{31}$$

$$t_{\theta_2} = \begin{bmatrix} -l_2 \sin(\theta_2) \\ l_2 \cos(\theta_2) \\ 1 \end{bmatrix} \tag{32}$$

$$t_{d_1} = \begin{bmatrix} \cos\theta_1 \\ \sin\theta_1 \\ 0 \end{bmatrix} \tag{33}$$

To assume the length of each link and prismatic part is 1, the magnitude of the elements of the volume of these tangent vectors are given by

$$\begin{aligned} t_{\theta_1} \cdot t_{\theta_1} &= 4\sin^2\theta_1 + 4\cos^2\theta_1 + 1 = 5 \\ t_{\theta_1} \cdot t_{\theta_2} &= 2\sin\theta_1 \sin\theta_2 + 2\cos\theta_1 \cos\theta_2 + 1 = 2\cos(\theta_1 - \theta_2) + 1 \\ t_{\theta_1} \cdot t_{\theta_3} &= -2\sin\theta_1 \cos\theta_1 + 2\cos\theta_1 \sin\theta_1 = 0 \\ t_{\theta_2} \cdot t_{\theta_1} &= 2\sin\theta_1 \sin\theta_2 + 2\cos\theta_1 \cos\theta_2 + 1 = 2\cos(\theta_1 - \theta_2) + 1 \\ t_{\theta_2} \cdot t_{\theta_2} &= \sin^2\theta_2 + \cos^2\theta_2 + 1 = 2 \\ t_{\theta_2} \cdot t_{\theta_3} &= -\sin\theta_2 \cos\theta_1 + \cos\theta_2 \sin\theta_1 = \sin(\theta_1 - \theta_2) \end{aligned}$$

$$
\begin{aligned}
t_{\theta_3} \cdot t_{\theta_1} &= -2\sin\theta_1\cos\theta_1 + 2\cos\theta_1\sin\theta_1 = 0 \\
t_{\theta_3} \cdot t_{\theta_2} &= -\sin\theta_2\cos\theta_1 + \cos\theta_2\sin\theta_1 = \sin(\theta_1 - \theta_2) \\
t_{\theta_3} \cdot t_{\theta_3} &= \cos^2\theta_1 + \sin^2\theta_1 = 1
\end{aligned} \tag{34}
$$

The magnitude of the volume by these vectors are given by

$$
\begin{vmatrix}
t_{\theta_1} \cdot t_{\theta_1} & t_{\theta_1} \cdot t_{\theta_2} & t_{\theta_1} \cdot t_{\theta_3} \\
t_{\theta_2} \cdot t_{\theta_1} & t_{\theta_2} \cdot t_{\theta_2} & t_{\theta_2} \cdot t_{\theta_3} \\
t_{\theta_3} \cdot t_{\theta_1} & t_{\theta_3} \cdot t_{\theta_2} & t_{\theta_3} \cdot t_{\theta_3}
\end{vmatrix}^{\frac{1}{2}}
$$

$$
= \begin{vmatrix}
5 & 2\cos(\theta_1 - \theta_2) + 1 & 0 \\
2\cos(\theta_1 - \theta_2) + 1 & 2 & \sin(\theta_1 - \theta_2) \\
0 & (\theta_1 - \theta_2) & 1
\end{vmatrix}^{\frac{1}{2}} \tag{35}
$$

If $x = \cos(\theta_1 - \theta_2)$, eq.(35) can be expressed as following equations

$$
\begin{aligned}
&\sqrt{10 - 5\sin^2(\theta_1 - \theta_2) - (2\cos(\theta_1 - \theta_2) + 1)^2} \\
&= \sqrt{10 - 5(1 - x^2) - (2x + 1)^2} \\
&= \sqrt{x^2 - 4x + 4} \\
&= |x - 2| \\
&= |\cos(\theta_1 - \theta_2) - 2|
\end{aligned} \tag{36}
$$

$$
\begin{aligned}
V &= \int_0^{2\pi}\left(\int_0^{2\pi}\left(\int_0^{d1}|\cos(\theta_1 - \theta_2) - 2|\,dd1\right)d\theta_1\right)d\theta_2 \\
&= 8\pi^2
\end{aligned} \tag{37}
$$

2.4.3 Motion Capability of P-R-P type

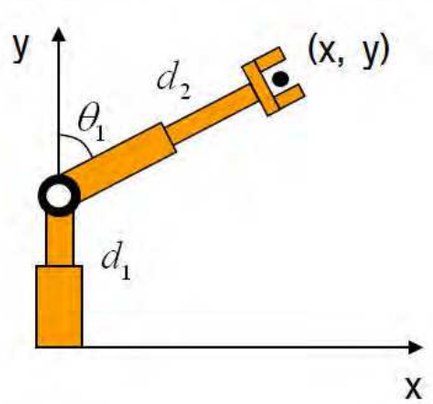

Fig. 14. P-R-P type manipulator

Finally, we consider the P-R-P type manipulator (Fig.14). This manipulator induces a parameterization of the manifold $R^2 \times 2\pi$ via the forward analysis. This yield.

$$\begin{aligned} x &= d_2 + \cos\theta_1 \\ y &= d_1 + d_2 \sin\theta_1 \\ \theta &= \theta_1 \end{aligned} \tag{38}$$

Assuming the revolute joint can rotate 2π radians, the volume element and motion capability of this manipulator is given by

$$V = \int_0^{d_1}\int_0^{d_2}\int_0^{2\pi} \left|\sin\theta_1\right| d\theta_1 ds_1 ds_2 = 4d_1 d_2$$

We can use this value of motion capabilities of each type to compare the average degree of joint. That is the relationship between this motion capability and the area of the manipulator's physical workspace. For a convenience of calculation, we assume that link length of each time is 1. First, motion capability of R-R-R type is, as stated above, 16π, and the physical workspace covers a circle of radius $l_1 + l_2 = 2$. Dividing this result by the area of the physical workspace of the robot yields

$$\frac{V_{RRR}}{\pi\left(2\cdot 1\right)^2} = 4\pi \tag{39}$$

Eq(39) shows that the R-R-R manipulator achieves a double covering its physical workspace and is able to rotate a body 2π radians about any point in this workspace. Similarly, we can calculate this value about R-P-R and P-R-P type.

$$\text{R-P-R type}: \quad \frac{V_{RPR}}{\pi\left(l_1 + d_1\right)^2} = \frac{V_{RPR}}{\pi\cdot 2^2} = \frac{8\pi^2}{4\pi} = 2\pi \tag{40}$$

$$\text{P-R-P type}: \quad \frac{V_{PRP}}{2l_1 l_2 + \pi {l_2}^2} = \frac{4l_1 l_2}{2l_1 l_2 + \pi {l_2}^2} = \frac{4}{2+\pi} \approx 0.78 \tag{41}$$

As a result, increasing the prismatic joint means decline of the motion capability of a manipulator.

3. Selection of Adequate Link Length Combinaion

Non-redundant planar manipulator is considered as shown in Fig.15.

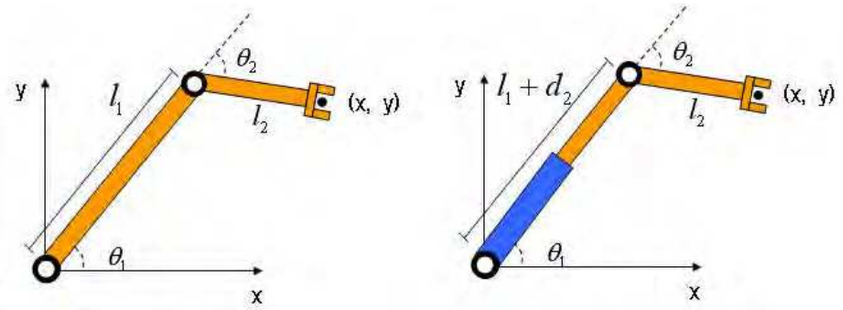

Fig. 15. Generalized planar manipulator

To deal with the simplest symbolic expressions, it is convenient to consider the Jacobian ${}^2J$ that correspond to task coordinates expressed in the second coordinate frame located at the manipulator end-effecter.

$$J \equiv {}^2J = \begin{bmatrix} l_1 \sin_2 & 0 \\ l_2 + l_1 \cos_2 & l_2 \end{bmatrix} \tag{42}$$

For this manipulator value decomposition (Golub and Van Loan 1989) of the Jacobian matrix have been derived in symbolic form (Kircanski and Boric 1993). Thus, the singular values σ_1 and σ_2 are given by

$$\sigma_{1,2} = \sqrt{\frac{l_1^2 + 2l_2^2 + 2l_1 l_2 c_2 \pm \sqrt{(l_1^2 + 2l_2^2 + 2l_1 l_2 c_2 - 4l_1^2 l_2^2 s_2^2)}}{2}} \tag{43}$$

It is obvious that $\sigma_1 \geq \sigma_2$ is always satisfied. One of the best measures of robot dexterity- condition number- is defined as the ratio of the maximum and minimum singular values. [9] Once the singular values have been derived symbolically, the condition number is also obtained symbolically as a function of the ratio between the link lengths k and the joint angle θ_2 .

$$k = \frac{l_1}{l_2} \tag{44}$$

$$\mu(k, \theta_2) = \frac{\sigma_1}{\sigma_2} = \sqrt{\frac{k^2 + 2 + 2kc_2 + \sqrt{(k^2 + 2 + 2kc_2)^2 - 4k^2 s_2^2}}{k^2 + 2 + 2kc_2 - \sqrt{(k^2 + 2 + 2kc_2)^2 - 4k^2 s_2^2}}} \tag{45}$$

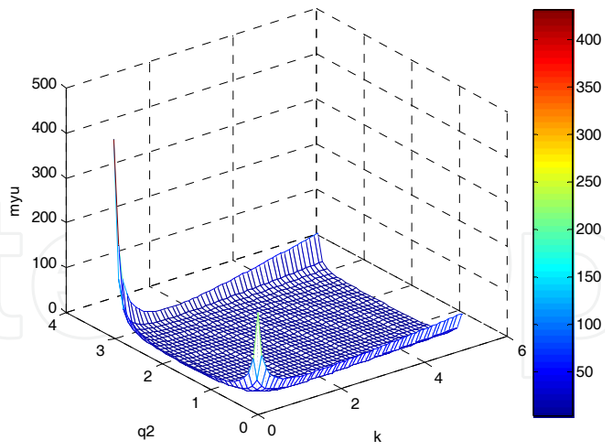

Fig. 16. Condition number versus joint angle and link length ratio

Fig.16 shows this relationship. The shaded zone at the contour graph designates the region where the condition number is less than 1.3. The isotropy condition means that the condition number has the optimal value of unity, that the two singular values are identical,

$$(k^2 + 2 + 2kc_2)^2 = 4k^2 s_2^2 \tag{46}$$

It can be satisfied only if $l_1 = l_2\sqrt{2}, \sin\theta_2 = \frac{\sqrt{2}}{2}, \cos\theta_2 = -\frac{\sqrt{2}}{2}$ (47)

The same result is obtained from the conditions that the rows of J must be mutually orthogonal and of equal lengths. Fig.17 shows the minimum condition number versus the link lengths ratio $k = l_1 / l_2$ for a family of 2-DOF planar manipulator.

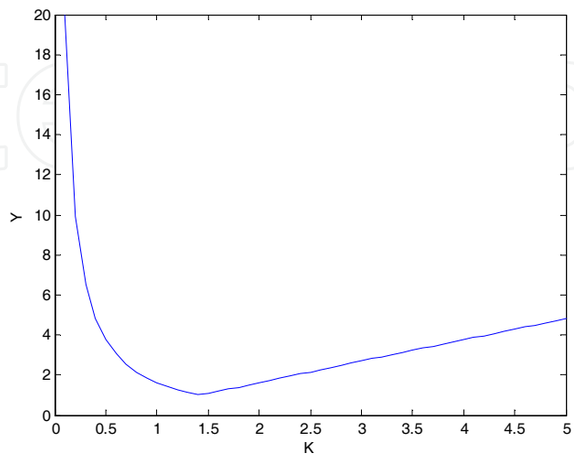

Fig. 17. The minimum condition number vs. the link lengths ratio $k = l_1 / l_2$

Fig. 17 is plotted by eq.(48)

$$\mu_{\min}(k) = \min_{q_2} \mu(k, q_2) = \sqrt{\frac{k^4 + 4 + \left|k^2 - 2\right|\sqrt{k^4 + 4}}{k^4 + 4 - \left|k^2 - 2\right|\sqrt{k^4 + 4}}} \tag{48}$$

Fig.18 shows the variation of the condition number with the joint angle θ_2 for several values of the link lengths ratio k. It is obvious not only that the optimal condition number of unity is achievable only if $k = \sqrt{2}$, but also that the condition number increases with θ_2 in vicinity of the isotropic configuration. Therefore, $k = \sqrt{2}$ can be a proclaimed value as the optimal 2-DOF planar manipulator design. This result, however, is opposed to the result of manipulability analysis of previous chapter. Therefore, robot designer has to choose the appropriate ratio of link lengths for his/her own purpose.

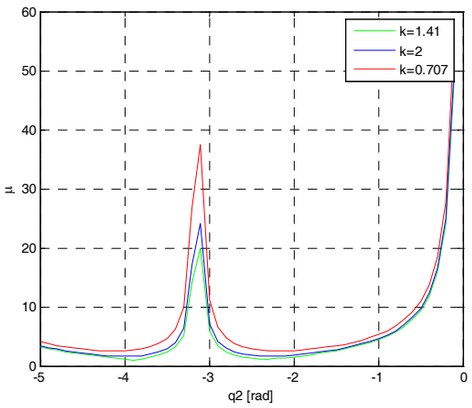

Fig. 18. The condition number with the joint angle θ_2 for several values of the link lengths ratio k

4. Conclusion

This paper introduces a design concept for a robot manipulator specific to the curtain wall installation task or any other similar task that is in a dominant task area with a full stretch, high manipulability and motion capability, etc. Fig.19 shows the results of this study. This design concept is based on the following assumptions.

1. The task was assumed to be curtain wall installation during the construction of a tall building.
2. The required DOF of the manipulator is six, with an unchangeable rotational base frame.
3. The end-effecter of the manipulator has a 3-DOF R-P-R type joint, which is also invariant.
4. The previous assumption makes this problem rather simple thus it was handled as a planar manipulator problem.

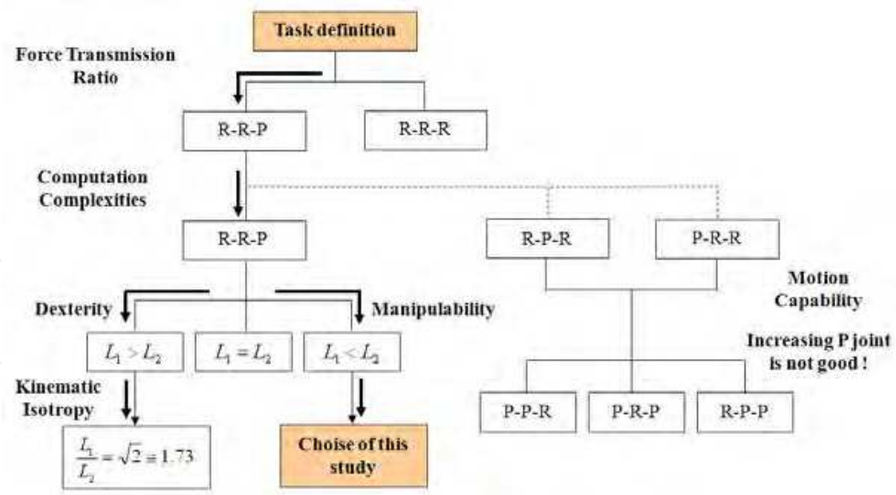

Fig. 19. Flowchart showing the decision process for determining the optimal design of a manipulator for the specified task.

The following figure illustrates the concept of a man-machine cooperation system for curtain wall installation based on the results of this study.

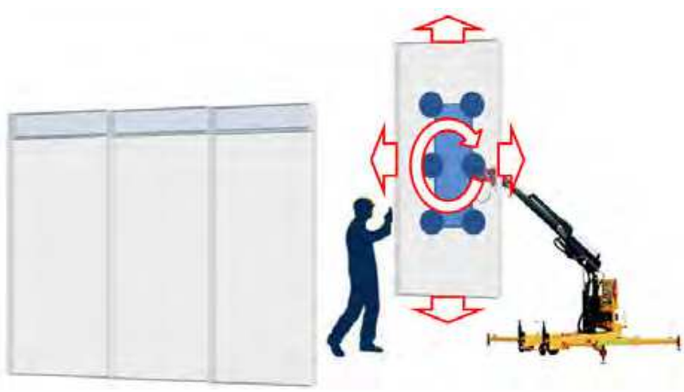

Fig. 20. Concept of an assistant manipulator for curtain wall installation

Acknowledgement

This work was supported by the Research Fund of Hanyang University (HYU-2009-T) and a grant from Construction Technology Innovation Program(CTIP) funded by Ministry of Land, Transportation and Maritime Affairs (MLTM),SRC/ERC program of MOST (grant #R11-2005-056-03003-0).

6. Reference

[1] SeungNam Yu, Seung Yeol Lee, Chang Soo Han, Kye Young Lee, Sang Heon Lee, "Development of the curtain wall installation robot: Performance and efficiency tests at a construction site", Autonomous Robots, Vol.22, No.3, pp.281~291, 2007

[2] Jin-u Lee, Chang-Baek Son, "An Analysis of Work Ratio for construction Curtain wall by Work Sampling Technique", The Korean Construction Society 2003, pp.519~522
[3] Seung-Nam Yu, Jong-Ho Choe, Seung-Yel Lee, Chang-Soo. Han, Kye-Young Lee, Sang-Heon Lee, "The Analysis of the Curtain Wall Installation Robot: Based on the Test in the Construction Processes", ISARC 2005, Ferrara, Italy, pp76, 2005
[4] John J. Craig, "Introduction to Robotics – Mechanics and Control, 3rd Edition", Addison Wesley, 2005
[5] Stephen L. Chiu, "Task Compatibility of Manipulator Postures", The International Journal of Robotics Research, Vol.7, No.5, 13-21, 1988
[6] Prasadkumar P. Bhangale, S. K. Saha, V. P. Agrawal, "Dynamic Model Based Selection Criterion for Robot Manipulators", Mutibody Dynamics 2003, Jorge A.C. Ambrósio(Ed.), IDMEC/IST, Lisbon, Portugal, July 1-4, 2003
[7] Tsuneo Yoshikawa, "Manipulability of Robotic Mechanisms", The international journal of Robotics Research, 1985, pp.3~4
[8] Udai Basavaraj, Joseph Duffy, "End-Effector Motion Capabilities of Serial Manipulators, The international journal of Robotics Research, 1993, pp132~137
[9] Manja Kircanski, "Kinematic Isotropy and Optimal Kinematic Design of Planar Manipulators and a 3-DOF Spatial Manipulator", The Int. Journal of Robotics Research", Vol.15, No.1, pp.61-77, 1996

Robot Manipulators New Achievements

Edited by Aleksandar Lazinica and Hiroyuki Kawai

ISBN 978-953-307-090-2
Hard cover, 718 pages
Publisher InTech
Published online 01, April, 2010
Published in print edition April, 2010

Robot manipulators are developing more in the direction of industrial robots than of human workers. Recently, the applications of robot manipulators are spreading their focus, for example Da Vinci as a medical robot, ASIMO as a humanoid robot and so on. There are many research topics within the field of robot manipulators, e.g. motion planning, cooperation with a human, and fusion with external sensors like vision, haptic and force, etc. Moreover, these include both technical problems in the industry and theoretical problems in the academic fields. This book is a collection of papers presenting the latest research issues from around the world.

InTech Europe
University Campus STeP Ri
Slavka Krautzeka 83/A
51000 Rijeka, Croatia
Phone: +385 (51) 770 447
Fax: +385 (51) 686 166
www.intechopen.com

InTech China
Unit 405, Office Block, Hotel Equatorial Shanghai
No.65, Yan An Road (West), Shanghai, 200040, China
中国上海市延安西路65号上海国际贵都大饭店办公楼405单元
Phone: +86-21-62489820
Fax: +86-21-62489821

IntechOpen